Effects of cyclosporin A pre-treatment combined with etomidate post-treatment on lung injury induced by limb ischemia-reperfusion in rats

Haibo Zou [iD] **and Xiaofeng Sun**

Abstract

Objectives: To investigate the influence of cyclosporin A (CsA) pre-treatment and etomidate (ETO) post-treatment on lung injury induced by limb ischemia-reperfusion (I/R) in rats.

Methods: Rats were randomly divided into five groups: sham, I/R, I/R+CsA, I/R+ETO, and I/R+CsA+ETO. Limb I/R lung injury was established by bilateral clamping of the femoral arteries for 2 hours. Following reperfusion for 3 hours, blood gas analysis was performed. Pathological changes were assessed using immunohistochemistry. The apoptosis index (AI) and wet/dry weight ratio (W/D) were calculated. Levels of Fas protein and FasL mRNA were assessed by western blotting and RT-PCR, respectively. Tumor necrosis factor (TNF)-α and interleukin (IL)-1β were detected by ELISA.

Results: I/R resulted in decreased PaO_2 but increased AI, W/D, Fas, FasL mRNA, TNF-α and IL-1β. Scattered punctate apoptosis and necrosis were observed by immunohistochemistry. Compared with the I/R group, the I/R+ETO and I/R+CsA groups showed increased SpO_2, decreased AI, W/D, Fas, FasL mRNA, TNF-α and IL-1β, and decreased numbers of apoptotic and necrotic cells. Combined treatment with CsA+ETO resulted in more dramatic changes in these parameters.

Conclusions: ETO post-treatment and CsA pretreatment reduced lung injury induced by limb I/R in rats. The mechanism may be related to synergistic inhibition of Fas/FasL signaling.

Central Hospital Affiliated to Shenyang Medical College, Shenyang City, Liaoning Province, China

Corresponding author:
Haibo Zou, Department of Anesthesiology, Central Hospital Affiliated to Shenyang Medical College, Tiexi District, Shenyang City 110024, Liaoning Province, China.
Email: 30618734@qq.com

Lung injury induced by limb ischemia-reperfusion (LILIR) is of high clinical interest. In-depth studies of ischemia-reperfusion (I/R) have found that in addition to tissues directly affected by I/R, distant organs may also be damaged.[1] Some studies showed that etomidate (ETO) can reduce injury associated with brain ischemia-reperfusion by down-regulating Fas/FasL.[2,3] Other studies showed that cyclosporin A (CsA) can reduce injury associated with myocardial ischemia-reperfusion by reducing the expression of FasL on the cell surface.[4] The membrane surface molecules Fas and its ligand FasL have a profound impact on the mechanism of apoptosis.[5] Our previous studies found that limb I/R could induce kidney and liver injuries in rats.[6,7] Based on these results, we wondered whether ETO post-treatment and CsA pre-treatment would affect Fas/FasL signaling during limb I/R in rats. Clinically, almost all patients undergoing lower limb surgery experience injuries caused by limb I/R. Therefore, it is necessary to better understand the mechanisms of limb I/R injuries in animal models. The aim of study was to investigate the synergistic effects of ETO post-treatment and CsA pre-treatment on limb I/R injuries in rats.

Materials and methods

Randomization

A random number table method was used to select animals and assign them to treatment groups.

Time and place

Time: 2019. Setting: Central Hospital Affiliated to Shenyang Medical College

Materials

Animal groups and LILIR model: A total of 150 adult male Sprague Dawley (SD) rats (6–8 months old, body weight 280–320 g; provided by the laboratory center of China Medical University) were randomly assigned to treatment groups. Rat cages were controlled at $24 \pm 1°C$ and 45% to 55% relative humidity. An incubator constructed from transparent and insulating materials was used to ensure natural alternation between day and night (12 hours/12 hours). All rats were given free access to food and drinking water. During and before the experiment rat cages were cleaned regularly. The 150 SD rats were randomly divided into five groups (n = 30 rats per group): sham, I/R, I/R+CsA, I/R+ETO, and I/R+CsA+ETO. The rat LILIR model was based on a previous study[8]. Prior to the model, all rats were fasted for 12 hours but had free access to drinking water. The rats were anesthetized with 3% sodium pentobarbital (40 mg/kg), then the right external jugular vein was catheterized to establish venous access. The femoral artery and femoral vein were separated. The femoral artery was clipped and closed near the inguinal ligament using a non-invasive micro artery clamp, inducing hind limb ischemia for 2 hours. The micro artery clamp was released and reperfusion proceeded for 3 hours. Blood flow was monitored using an ES-1000 SPM ultrasonic blood flow instrument (Hayashi Denki, Osaka, Japan). Undetectable blood flow was taken as an indicator of ischemia, and detectable blood flow as an indicator of reperfusion. During the experiment, normal saline ($1.5 \, mL \, kg^{-1} \, h^{-1}$) was infused intravenously. The sham group underwent open surgery, but no I/R was induced. The I/R group experienced LILIR. The I/R+CsA group received intravenous injections of CsA (10 mg/kg, Novartis AG, Basel, Switzerland) once a day for 1 week prior to LILIR. The I/R+ETO group received ETO (1 mg/kg, Enhua Co., Ltd., Jiangsu, China) intravenously 2 hours following LILIR. The I/R+CsA+ETO group received pre-treatment with CsA,

underwent LILIR, then received post-treatment with ETO. The sham group and I/R groups were injected with the same volume of physiological saline instead of CsA or ETO. At the end of the experiment, the rats were sacrificed by exsanguination.

Experimental methods

Ethics. The animal study was approved by the local Ethics Board of the Central Hospital of Shenyang Medical College (Shenyang City, China).

Blood gas analysis. Blood (3 mL) was obtained from the carotid artery following 3 hours of limb reperfusion. Blood gas analysis was conducted immediately using a Gem Premier 3000 Blood Gas Analyzer (LeiCheng Trading Co., Ltd., Nanjing City, China) and PaO_2 was recorded.

Biochemical indexes and wet/dry weigh ratio (W/D). Levels of tumor necrosis factor (TNF)-α and interleukin (IL)-1β were assessed using an ELISA kit (Abcam Co., Cambridge, UK). Following limb reperfusion for 3 hours, tissue from the upper pole (1 cm^3) of the left lung was used to produce 10% lung tissue homogenate. For ELISA, lung tissue homogenates (100 μL/well) were added, then plates were sealed and incubated at 37°C in the dark for 2 hours. The plates were washed, a biotinylated antibody (100 μL/well) was added, and the plates were re-sealed and incubated at room temperature for 1 hour. The plates were washed again and a horseradish peroxidase-conjugated secondary antibody (100 μL/well) was added and incubated at room temperature for 20 minutes. The plates were washed a final time, developer (100 μL/well) was added, and the plates were incubated in the dark for 20 minutes. The reaction was terminated with stop solution (50 μL/well), the plates were gently agitated, and then the absorbance at 450 nm was measured. Absorbance values from blank wells were subtracted from the average values for experimental wells. Standard curves were constructed and used to calculate TNF-α and IL-1β concentrations.

For calculation of W/D, the lower pole tissue of the right lung (1 cm^3) was obtained and washed with 4°C normal saline. Residual blood was removed and surface water was dried with filter paper. The wet weight (W) was measured, then the lung tissue was dried at 80°C for 48 hours. The dry weight (D) was measured and then W/D was calculated.

Immunohistochemistry. The streptavidin–biotin complex (SABC) method was used and the experimental steps were carried out according to the manufacturer's instructions. 3,3′-Diaminobenzidine (DAB) was used to stain samples and positive expression was classified as brown cytoplasm. A sample of the middle pole lung tissue (1 cm^3) was obtained from the right lung. The sample was dewaxed, hydrated, washed twice with phosphate-buffered saline (PBS) for 5 minutes, then incubated at room temperature in PBS containing 3% H_2O_2 for 5 to 10 minutes. The sample was washed with distilled water three times then antigen retrieval was performed. The sample was washed with PBS for 5 minutes, then normal sealing solution was added by dripping and incubated at room temperature for 20 minutes. Excess liquid was removed. Primary antibody (1:100 dilution, Abcam) was added and incubated at room temperature for 1 hour. After washing with PBS three times for 2 minutes, biotinylated secondary antibody (1:100 dilution, Abcam) was added and incubated at 20 to 37°C for 20 minutes. After washing with PBS three times for 2 minutes, SABC reagent was added and incubated at 20 to 37°C for 20 minutes, then the plates were washed with PBS four times for 5 minutes.

DAB color was developed using a DAB color development kit.

After washing with distilled water, hematoxylin was added and the samples were set aside for 2 minutes. The samples were then treated with hydrochloric acid and alcohol, dehydrated, sealed and examined under the microscope. Brown-stained cells were classified as positive. Five visual fields were randomly selected from each section, and 100 cells were counted from each visual field. The ratio of brown-stained cells to these 100 cells (RBS) was calculated.

Hoechst33258 staining. A sample of right upper lung tissue (1 cm^3) was obtained, embedded and sectioned routinely. The sections were washed with PBS, stained for 5 minutes with Hoechst33258 staining solution (0.5 mL, AAT Bioquest Inc, CA, USA), then washed again with PBS. The sections were placed on slides, antiquenching sealing solution was added, and the slide was covered. The slides were observed by fluorescence microscopy under 200× magnification. Using a BX-41 microscope (Olympus Corporation, Tokyo, Japan), normal nuclei can be observed as round and dark blue. By contrast, the chromatin of apoptotic cells is pyknotic, and their nuclei are dense or fragmented with a bright white color. Cells with dense or white-bright nuclei were counted. Five visual fields were randomly selected from each section, and 100 cells were counted from each visual field. The ratio of apoptotic cells among these 100 cells was taken as the apoptotic index (AI).

Fas protein expression. Western blotting was used to detect Fas protein expression in lung tissue. Lung tissue (1 cm^3) was obtained from the lower pole of the right lung. Residual blood was washed with 4°C normal saline, then the samples were dried with filter paper and 10% tissue homogenate was prepared. Total protein was extracted by centrifugation and protein concentrations were assessed using a DYY-6B electrophoresis instrument (Liuyi Instrument Factory, Beijing, China). Following SDS-PAGE, electrophoretic transfer to polyvinylidene difluoride membranes, and blocking, rabbit anti-rat Fas polyclonal antibody (Abcam) and rabbit anti-rat β-actin polyclonal antibody (Abcam) were added and incubated at 4°C overnight. Alkaline phosphatase conjugated secondary antibody (Sigma) was added, incubated at room temperature for 2 hours, and then substrate was applied for color scanning. The blots were imaged using the Scion Image Analysis System (Apple, Cupertino, CA, USA). Fas expression was calculated by densitometry by comparison with expression of β-actin.

FasL mRNA expression. RT-PCR was used to detect the expression of FasL mRNA in lung tissue. Lung tissue (1 cm^3) from the lower pole of the left lung was used to prepare 10% lung tissue homogenate. Total RNA was extracted using Trizol (Sigma, St. Louis, MO, USA), reverse transcribed into cDNA, and then amplified by PCR (Eppendorf, Hamburg, Germany). The sequences of primers were as follows: FasL mRNA (395 bp, Bao Bioengineering Co., Ltd. Dalian City, China) upstream primer 5′-ACGACACGGACAGC-3′, downstream primer 5′-GATCACGCGAG GAGCAC-3′; and β-actin (198 bp): upstream primer 5′-CATCTCGGATGCA CAG-3′, downstream primer 5′-GGACC CGTAGCACG-3′. The reaction conditions for FasL mRNA RT-PCR were: 94°C predenaturation for 2 minutes; 35 cycles of 95°C for 45 s, 57°C 45 s, 72°C for 60 s; 72°C extension for 5 minutes. The reaction conditions for β-actin were: predenaturation at 94°C for 2 minutes, 30 cycles of 94°C for 40 s, 58°C for 40 s, 72°C for 60 s; 72°C extension for 5 minutes. The PCR products were analyzed by 2%

agarose gel electrophoresis and ethidium bromide staining. The expression level of FasL mRNA was assessed based on the relative densitometry of the FasL and β-actin PCR products using the Scion Image Analysis System.

Statistical methods

SPSS version 13.0 software (SPSS Inc., Chicago, IL, USA) was used for all statistical analyses. Data were expressed as means ± standard deviations (x ± s). Differences between groups were assessed using the independent sample t-test, single factor analysis of variance and Fisher's least significant difference test. Correlational analyses were also performed. Values of $P < 0.05$ were considered statistically significant.

Results

Analysis of the number of experimental animals

All 150 rats survived the procedures and results were available for analysis.

TNF-α, IL-1β, and PaO$_2$

Compared with the sham group, levels of TNF-α and IL-1β were increased and PaO$_2$ was decreased in the I/R group ($P = 0.032$). Compared with the I/R group, levels of TNF-α and IL-1β decreased and PaO$_2$ was increased in the I/R+CsA and

I/R+ETO groups ($P = 0.016$). Compared with both the I/R+CsA and I/R+ETO groups, levels of TNF-α and IL-1β were further decreased and PaO$_2$ was further increased in the I/R+CsA+ETO group ($P = 0.027$) (Table 1).

Immunohistochemistry

Under the light microscope, the lung cells of the sham group rats were orderly, and few leukocytes were observed infiltrating into the alveoli. In the I/R group, many inflammatory cells infiltrated into the alveoli. An increased number of necrotic cells with brownish yellow staining were observed and occasionally aggregated. In the I/R+CsA and the I/R+ETO groups, changes were similar: necrotic foci with dense punctate staining were observed, and inflammatory cells were decreased. In the I/R+CsA+ ETO group, necrotic cells were occasionally seen, and the number of inflammatory cells decreased in the alveoli and pulmonary interstitium was reduced (Figure 1 and Table 2).

Hoechst33258 staining and AI

Compared with the sham group, the AI was increased in the I/R group ($P = 0.021$). Compared with the I/R group, the AI was decreased in the I/R+CsA and I/R+ETO groups ($P = 0.034$). Compared with the I/R+CsA and I/R+ETO groups, the AI was further decreased in the I/R+CsA+

Table 1. Comparison of TNF-α, IL-1β, W/D and PaO$_2$ in each group (n = 30, x + s).

Group	TNF-α (mg/mL)	IL-1β (ug/L)	W/D	PaO$_2$ (mmHg)
Sham	1.21 ± 0.05	0.42 ± 0.02	2.3 ± 0.2	97 ± 3
I/R	3.96 ± 0.23[a]	1.43 ± 0.17[a]	5.3 ± 0.4[a]	75 ± 3[a]
I/R+CsA	1.93 ± 0.46[b]	0.97 ± 0.03[b]	4.1 ± 0.5[b]	92 ± 2[b]
I/R+ETO	2.12 ± 0.32[c]	0.88 ± 0.03[c]	3.8 ± 0.4[c]	90 ± 3[c]
I/R+CsA+ETO	0.71 ± 0.25[d]	0.29 ± 0.05[d]	2.6 ± 0.7[d]	96 ± 2[d]

[a]$P < 0.05$ compared with sham group; [b]$P < 0.05$ and [c]$P < 0.05$ compared with I/R group; [db]$P < 0.05$ and [dc]$P < 0.05$ compared with I/R+CsA group and I/R+ETO groups, respectively.
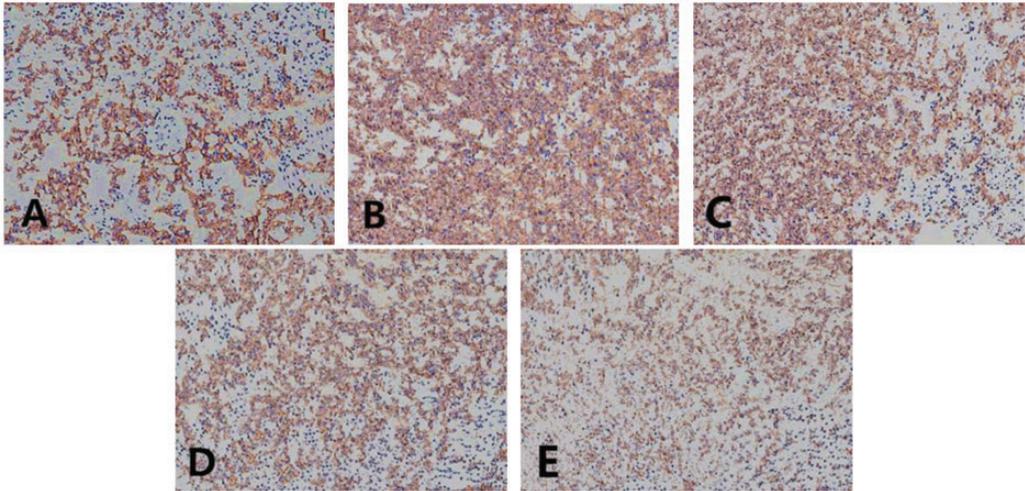
Figure 1. Morphological structures of lung immunohistochemical sections in each group by light microscopy (200×). A: Sham group; B: I/R group; C: I/R+CsA group; D: I/R+ETO group; E: I/R+CsA+ETO group.

Table 2. Comparison of AI and RBS in each group (n = 30, x + s).

	Sham	I/R	I/R+CsA	I/R+ETO	I/R+CsA+ETO
AI	41.39 ± 4.62	63.21 ± 3.69[a]	52.43 ± 3.55[b]	57.09 ± 4.87[c]	39.01 ± 4.27[d]
RBS	4 ± 1	11 ± 2[a]	8 ± 1[b]	7 ± 2[c]	5 ± 2[d]

[a]$P < 0.05$ compared with sham group; [b]$P < 0.05$ and [c]$P < 0.05$ compared with I/R group; [db]$P < 0.05$ and [dc]$P < 0.05$ compared with I/R+CsA and I/R+ETO groups, respectively.

ETO group (P = 0.019) (Figure 2 and Table 2).

Comparison of Fas protein expression

Compared with the sham group, Fas protein expression was increased in the I/R group (P = 0.025). Compared with the I/R group, Fas expression was decreased in the I/R+CsA and I/R+ETO groups (P<0.033). Compared with the I/R+CsA and I/R+ETO groups, Fas expression in the I/R+CsA+ETO group was further decreased (P = 0.017) (Table 3 and Figure 3).

Comparison of FasL mRNA

Compared with the sham group, FasL mRNA levels in the I/R group were increased (P = 0.024). Compared with the I/R group, FasL mRNA levels in the I/R+CsA and I/R+ETO groups were decreased (P = 0.013). Compared with the I/R+CsA and I/R+ETO groups, FasL mRNA levels in the I/R+CsA+ETO group were further decreased (P = 0.021) (Table 3 and Figure 4).

Discussion

As minimally invasive surgery becomes more common, microscopy is applied more and more frequently. A clear surgical field becomes the most basic requirement that minimally invasive surgeries must meet.[9] In hand and foot surgeries, the application of tourniquets can meet the requirements of surgeons for clarity of surgical field, but collateral injury occurs from
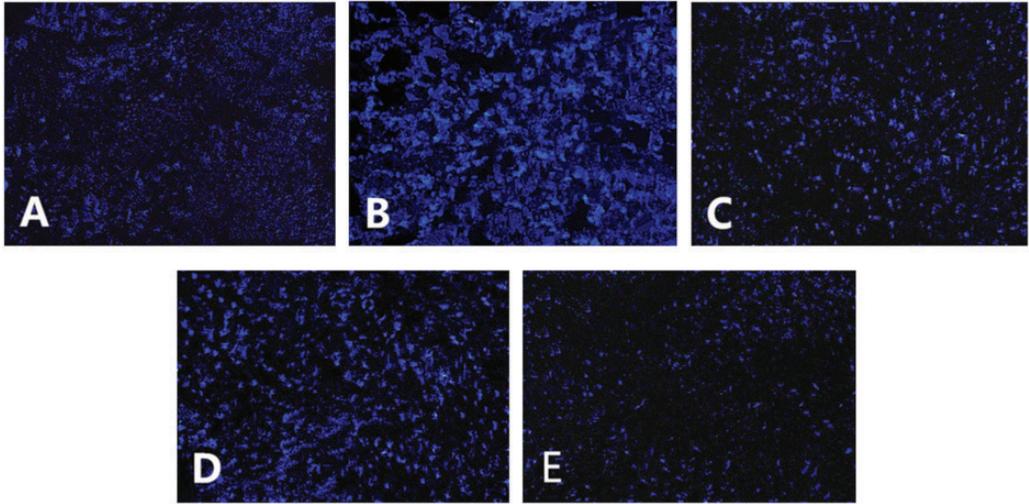
Figure 2. Comparison of Hoechst33258 staining in the lung tissues of each group (200×).

Table 3. Comparison of relative amount of Fas and FasL mRNA in each group (n = 30, x + s).

	Sham	I/R	I/R+CsA	I/R+ETO	I/R+CsA+ETO
Fas	6.87 ± 1.31	13.28 ± 1.92[a]	9.91 ± 1.57[b]	10.97 ± 1.16[c]	7.85 ± 1.56[d]
FasL mRNA	0.31 ± 0.02	1.09 ± 0.02[a]	0.56 ± 0.05[b]	0.67 ± 0.03[c]	0.41 ± 0.07[d]

[a]$P < 0.05$ compared with sham group; [b]$P < 0.05$ and [c]$P < 0.05$ compared with I/R group; [db]$P < 0.05$ and [dc]$P < 0.05$ compared with I/R+CsA and I/R+ETO groups, respectively.
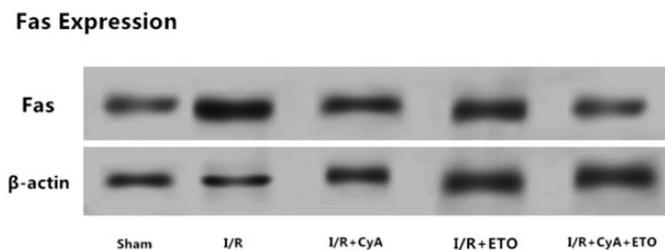
Fas Expression

Figure 3. Comparison of Fas protein expression in the lung tissues of each group.

limb I/R.[10,11] Earlier studies showed that I/R of the hind limbs in rats can lead to lung injury at distance sites. The mechanisms of injury are diverse, with no unified theory.[12] The Fas protein plays a major role in apoptosis.[13,14] Whether Fas protein and its ligand FasL are involved in LILIR was unclear. The purpose of this study was to study the synergistic effects of CsA pretreatment and ETO post-treatment on LILIR and the dependence of these effects on Fas/FasL.

FasL can bind the death receptor Fas, which induces apoptosis during the development of T-lymphocytes.[15,16] Fas and its ligand FasL have been thoroughly studied

FasL mRNA Expression

β-actin Expression
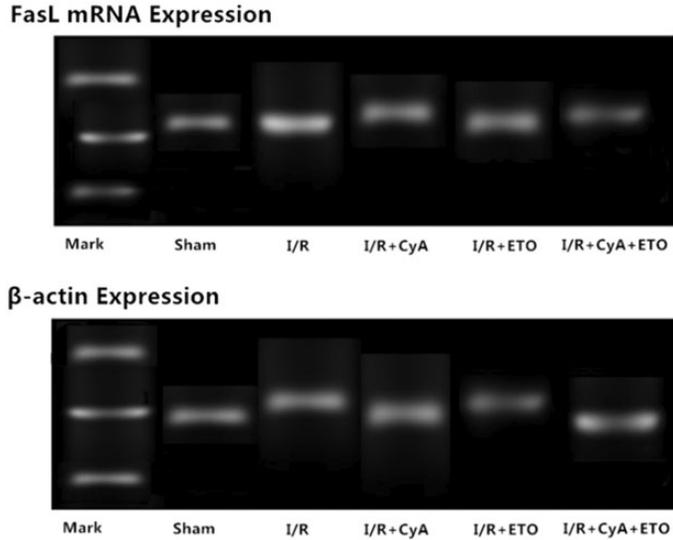
Figure 4. Comparison of FasL mRNA levels in the lung tissues of each group.

with a profound impact on our understanding of the mechanisms of apoptosis.[17–19]

CsA is a cyclic peptide comprising 11 amino acids. It is an active metabolite of fungi in soil and has strong immunosuppressive effects.[20–22] CsA can reversibly and selectively alter the function of T-lymphocytes, prevent the transcription of lymphokine genes, interfere with signaling,[19] inhibit release of IL-2, interferon and other immune factors, alter humoral and cellular immunity, inhibit the killing activity of natural killer cells, and inhibit the differentiation and proliferation of lymphocytes.[23,24]

ETO is used for general anesthesia and is a safe imidazole derivative. Inhibition of respiratory and circulatory functions during induction of general anesthesia with ETO is relatively slight.[24] Some studies have shown that ETO pre-treatment can reduce the expression of Bax protein during LILIR in rats, mediating a protective effect.[17] ETO may play a protective role in reperfusion injury by activating gamma-aminobutyric acid receptors, increasing the permeability of the cell membrane to Cl ions and preventing depolarization the cell

membrane.[25] In addition, the N-methyl-D-aspartate receptor and the Ca^{2+}-channel are voltage dependent; inhibition of cell membrane depolarization leads to decreased Ca^{2+} influx and decreased cellular oxygen consumption. Therefore, ETO can increase the tolerance of cells to ischemia-reperfusion injury.[2,26]

Compared with the sham group, Fas, FasL mRNA and other injury indexes were increased, while PaO_2 was decreased in the I/R group. This suggested that establishment of the rat LILIR model was successful. We speculate that the mechanism of lung injury is probably related to Fas/FasL. Compared with the I/R group, Fas and FasL mRNA decreased while PaO_2 increased in the I/R+CsA and I/R+ETO groups. This suggested that both CsA pre-treatment and ETO post-treatment can reduce lung injury. The protective effects of CsA pre-treatment and ETO post-treatment were associated with inhibition of Fas/FasL. Compared with the I/R+CsA and I/R+ETO groups, Fas, FasL mRNA and other injury indexes were further decreased and PaO_2 was

further increased. It was previously shown that CsA pre-treatment can down-regulate the expression of FasL protein on the cell surface, thus inhibiting Fas/FasL signaling.[27] Based on these results, we conclude that CsA pretreatment and ETO post-treatment may have synergistic protective effects against LILIR in rats.

In conclusion, our results showed that both CsA pretreatment and ETO post-treatment can reduce LILIR in rats. The mechanism may be related to down-regulation of Fas/FasL expression. In addition, CsA pretreatment and ETO post-treatment have synergistic protective effects against LILIR in rats.

Declaration of conflicting interest

The authors declare that there is no conflict of interest.

ORCID iD

Haibo Zou ⓘ https://orcid.org/0000-0002-8442-8113

References

1. Liu S, Zhang XP, Han NN, et al. Pretreatment with low dose etomidate prevents etomidate-induced rat adrenal insufficiency by regulating oxidative stress-related MAPKs and apoptosis. *Environ Toxicol Pharmacol* 2015; 39: 1212–1220.

2. Zhu Y, Yin X, Li J, et al. Overexpression of microRNA-204-5p alleviates renal ischemia-reperfusion injury in mice through blockage of Fas/FasL pathway. *Exp Cell Res* 2019; 381: 208–214.

3. Cui J, Wei C, Deng L, et al. MicroRNA-143 increases cell apoptosis in myelodysplastic syndrome through the Fas/FasL pathway both *in vitro* and *in vivo*. *Int J Oncol* 2018; 53: 2191–2199.

4. Badalzadeh R, Azimi A, Alihemmati A, et al. Chronic type-I diabetes could not impede the anti-inflammatory and anti-apoptotic effects of combined postconditioning with ischemia and cyclosporine A in myocardial reperfusion injury. *J Physiol Biochem* 2017; 73: 111–120.

5. Fuping Z, Wuping L, Linhua W, et al. Tao-Hong-Si-Wu decoction reduces ischemia reperfusion rat myoblast cells calcium overloading and inflammation through the Wnt/IP3R/CAMKII pathway. *J Cell Biochem* 2018; 120: 13095–13106.

6. Yue S and Yonghe C. Effects of Xinfeng capsule on the Fas/FasL-mediated apoptotic pathway in patients with rheumatoid arthritis. *J Tradit Chin Med* 2018; 38: 601–609.

7. Tsaroucha AK, Valsami G, Kostomitsopoulos N, et al. Silibinin effect on Fas/FasL, HMGB1, and CD45 expressions in a rat model subjected to liver ischemia-reperfusion injury. *J Invest Surg* 2018; 31: 491–502.

8. Zheng MX, Song D, Luo ZY, et al. Effect of puerarin on expression of Fas/FasL mRNA in pulmonary injury induced by ischemia-reperfusion in rabbits. *Nat Prod Commun* 2015; 10: 252–256.

9. Chen L, Liang X, Tan X, et al. Safety and efficacy of combined use of propofol and etomidate for sedation during gastroscopy: systematic review and meta-analysis. *Medicine (Baltimore)* 2019; 98: e15712.

10. Jung YK, You SY, Kim SY, et al. Simultaneous determination of etomidate and its major metabolite, etomidate acid, in urine using dilute and shoot liquid chromatography-tandem mass spectrometry. *Molecules* 2019; 24: 4459.

11. Kim SK, Kang SW, Jin SA, et al. Protective effect of citric acid against hepatic ischemia reperfusion injury in Sprague-Dawley rats. *Transplant Proc* 2019; 51: 2823–2827.

12. Zhao DJ, Jianjuan K, Peipei G, et al. Quercetin improves blood-brain barrier dysfunction in rats with cerebral ischemia reperfusion via Wnt signaling pathway. *Am J Transl Res* 2019; 11: 4683–4695.

13. Hou H, Wang Y, Li Q, et al. Corrigendum to: The role of RIP3 in cardiomyocyte necrosis induced by mitochondrial damage of myocardial ischemia reperfusion. *Acta Biochim Biophy Sin* 2019; 51: 877.

14. Ganesh T, Zakher E, Estrada M, et al. Assessment of microvascular dysfunction in acute limb ischemia reperfusion injury. *J Magn Reson Imaging* 2019; 49: 1174–1185.

15. Drysch M, Wallner C, Schmidt SJ, et al. An optimized low-pressure tourniquet murine hind limb ischemia reperfusion model: Inducing acute ischemia reperfusion injury in C57BL/6 wild type mice. *PLoS One* 2019; 14: e0210961.

16. Keating S, Sage A, Ambrisko T, et al. The effect of midazolam or lidocaine prior to etomidate induction on cardiorespiratory function, intraocular pressure, and cortisol production in healthy dogs. *Vet Anaesth Analg* 2019; 46: 831(e8-e9).

17. Li R, Fan L, Ma F, et al. Effect of etomidate on the oxidative stress response and levels of inflammatory factors from ischemia-reperfusion injury after tibial fracture surgery. *Exp Ther Med* 2017; 13: 971–975.

18. Jimbo H, Nagai H, Fujiwara S, et al. Fas-FasL interaction in cytotoxic T cell-mediated vitiligo: the role of lesional expression of tumor necrosis factor-α and interferon-γ in Fas-mediated melanocyte apoptosis. *Exp Dermatol* 2020; 29: 61–70.

19. Guo Y, Wang W, Chen Y, et al. Continuous gibberellin A3 exposure from weaning to sexual maturity induces ovarian granulosa cell apoptosis by activating Fas-mediated death receptor signaling pathways and changing methylation patterns on caspase-3 gene promoters. *Toxicol Lett* 2020; 319: 175–186.

20. Oliveira ACC, Módolo NSP, Domingues MAC, et al. Effects of cyclosporine on ischemia-reperfusion injuries in rat kidneys. An experimental model. *Acta Cir Bras* 2019; 34: e201900806.

21. Zhang Y, Cao M, Wu Y, et al. Improvement in mitochondrial function underlies the effects of ANNAO tablets on attenuating cerebral ischemia-reperfusion injuries. *J Ethnopharmacol* 2020; 246: 112212.

22. Wang M, Niu A, Gong Z, et al. PEG-amino acid-przewaquinone a conjugations: synthesis, physicochemical properties and protective effect in a rat model of brain ischemia-reperfusion. *Bioorg Med Chem Lett* 2020; 30: 126780.

23. Li J, Yan Z and Fang Q. A mechanism study underlying the protective effects of cyclosporine-A on lung ischemia-reperfusion injury. *Pharmacology* 2017; 100: 83–90.

24. Pottecher J, Kindo M, Chamaraux-Tran TN, et al. Skeletal muscle ischemia-reperfusion injury and cyclosporine A in the aging rat. *Fundam Clin Pharmacol* 2016; 30: 216–225.

25. Yaqiin X, Xing L and Juan Z. Rosuvastatin reduces myocardial ischemia-reperfusion injury by inhibiting miR-155. *Int J Clin Exp Med* 2019; 12: 7975–7984.

26. Xu D, Wang B, Chen P, et al. c-Myc promotes tubular cell apoptosis in ischemia-reperfusion-induced renal injury by regulating c-FLIP and enhancing Fas/FasL-mediated apoptosis pathway. *Acta Pharmacol Sin* 2019; 40: 1058–1066.

27. Jinan W and Xiuwei L. Chamaejasmine induces apoptosis in human non-small cell lung cancer A549 cells through increasing the Bax/Bcl-2 ratio, caspase-3 and activating the Fas/FasL. *Minerva Med* 2019; 31: 237–245.